Generation of entangled photon pairs by semiconductor quantum dots in a structure of quantum cellular automata

2007 J. Phys.: Condens. Matter 19 326215

(http://iopscience.iop.org/0953-8984/19/32/326215)

IOP PUBLISHING JOURNAL OF PHYSICS: CONDENSED MATTER

J. Phys.: Condens. Matter **19** (2007) 326215 (12pp) doi:10.1088/0953-8984/19/32/326215

Generation of entangled photon pairs by semiconductor quantum dots in a structure of quantum cellular automata

M Feng[1,2], J H An[3,4] and W M Zhang[2,3]

[1] State Key Laboratory of Magnetic Resonance and Atomic and Molecular Physics, Wuhan Institute of Physics and Mathematics, Chinese Academy of Sciences, Wuhan 430071, People's Republic of China
[2] Department of Physics and Center for Quantum Information Science, National Cheng Kung University, Tainan 70101, Republic of China
[3] National Center for Theoretical Science, Tainan 70101, Republic of China
[4] Department of Modern Physics, Lanzhou University, Lanzhou 730000, People's Republic of China

E-mail: mangfeng1968@yahoo.com, anjh@phys.ncku.edu.tw and wzhang@mail.ncku.edu.tw

Received 11 June 2007, in final form 26 June 2007
Published 17 July 2007
Online at stacks.iop.org/JPhysCM/19/326215

Abstract

We propose a unique scheme to generate entangled photon pairs by six semiconductor quantum dots in a structure of quantum cellular automata. By means of interdot electronic tunneling, single-electron spin manipulation, and auxiliary excitons, we can convert the entanglement from the charge degrees of freedom of the electrons to the spin degrees of freedom of the electrons, and then to the polarization of the photons. Our scheme presents a source of entangled photon pairs without using spin–spin coupling, which could work repeatedly, deterministically and efficiently. Both the experimental challenge and the feasibility with present technologies are discussed. In comparison with former relevant work, our proposal not only gives an alternative method to generate entangled photons, but is applicable to other quantum information processing tasks with free electrons.

1. Introduction

Due to their engineerable properties and the potential for scalability, semiconductor quantum dots (SQDs) have been considered as an excellent candidate for physical implementation of quantum information. Besides application in quantum gatings based on the spin or charge degrees of freedom, SQDs are also good sources for single photons and entangled photon pairs.

Entangled photons are essential to quantum communication, quantum cryptography, and linear optical quantum computing. There have been some proposals and experiments for creating entangled photons, for example, using atomic cascade decay [1], parametric down

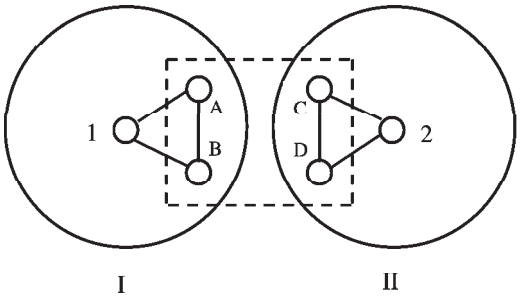

Figure 1. Schematic of our design for generating entangled photons, where the big and small circles represent, respectively, the microcavities and the SQDs. The lines between the SQDs mean the availability of interdot tunneling or transition, and the four dots A, B, C, and D in a dashed square box constitute a QCA.

conversion in nonlinear crystals [2], beam splitters [3] and exciton emission in SQDs [4–11]. Although the production rates and the collection rates of the entangled photons are still much lower than our expectation, once the entangled photons were prepared, some excellent experiments could be achieved [12–14]. On the other hand, entangled photons are essential to quantum computing with linear optical elements [15], particularly to a future quantum network based on local qubit subsystems. Since photons are flying qubits, the entanglement mapping from the photons to distant static qubits is a good way for quantum information transfer. We have noticed various proposals [16, 17] and a very recent experiment [18] to entangle atoms by detecting the entangled photons from beam splitters, which construct the quantum information channel between distant locations.

In this paper, we focus on generation of entangled photon pairs by SQDs in a structure of quantum cellular automata (QCA) [19]. As mentioned above, biexciton emission has usually been employed to produce entangled photon pairs [4]. However, due to the asymmetry from the electron–hole exchange interaction, the resulting level splitting makes entanglement unavailable in the present experiments [20, 21]. So generation of entangled photons by means of biexcitons must involve some tricks [5–7, 10, 11]. Here we will consider an alternative for entangling photon pairs. The trick we will employ is the recent finding that the independence between spin and charge degrees of freedom of electrons is essential to free electron quantum computing [22–24]. We will put SQDs in a QCA structure and try to produce entangled photons by means of electron tunneling. We have noticed recent experiments for coherent tunneling of the excess electrons between SQDs [25–27]. The conduction electrons can be considered as free electrons, based on which we can carry out free electron–spin quantum computing. As the key point of free electron quantum computing is using the technology of spin-to-charge conversion, detecting electron charge [22] or entangling charge states [23] would yield entanglement in the spin degrees of freedom. We will generate entangled photon pairs by using the idea of free electron quantum computing in [23].

Specifically, we consider six SQDs in a structure of QCA, as shown in figure 1, where the lines indicate the possibility of interdot tunneling and the four dots inside the dashed-line box constitute the QCA. QCA was originally proposed as a transistorless alternative to digital circuit devices at the nanoscale [28]. Quantum mechanically, when a QCA is charged with two electrons, the Coulomb repulsion would yield these two electrons to occupy coherently two antipodal sites, called the two allowed charge polarizations, denoted by $P = \pm 1$, respectively. By elaborately applying external bias voltages to adjust the splitting of the two charge polarizations [19], we could have the charged states to be entangled [29], based

on which an entanglement of electron spins could also be achieved without using spin–spin interaction [23].

For our purpose to generate entangled photons, we consider that the SQDs are embedded in two identical microcavities, respectively, and that each microcavity involves two modes, i.e., σ_+ and σ_-. We will discuss later that the microcavities are not essential to our proposal, although they are helpful for collecting generated photons. To clarify, we label the SQDs A, B, and 1 in the cavity I, and the SQDs C, D, and 2 in the cavity II. Dots 1 and 2 are initially charged with each containing a single excess electron in the conduction band, and there is no electron initially in the conduction bands of other dots. The interdot transition between dot 1 or 2 and other dots is made by switching on/off the bias voltages. The favorable features of our proposal include: (1) the spin entanglement is originally generated by charge degrees of freedom of the electrons in the SQDs, without using spin–spin coupling [23]. This is due to the relatively large spacing between SQDs, which makes the spin–spin coupling negligible. With this design, our scheme could be carried out very quickly, and the experimental challenge for controlling spin–spin coupling is removed; (2) the entanglement is then mapped from the spin degrees of freedom of the electrons to the photon polarization states in two cavity modes. Due to the long decoherence time of the spin and the efficiency of the entanglement conversion between electrons and photons, the generated entanglement of the photons would be of high fidelity; (3) we are able to prepare full Bell states of the entangled photons, which depends on the initial states and the operations on individual electrons in conduction bands, because our scheme is deterministic.

In what follows, we will present our scheme in section 2, and then discuss the experimental feasibility and challenge of our scheme in section 3. The last section contains the conclusion, and some detailed deduction can be found in appendices A and B.

2. Our scheme

Since the charge and spin degrees of freedom are independent for an electron, to be concise, we will below only write down the spin degrees of freedom, but denote by subscripts charge degrees of freedom. If we suppose to have initially $|\varphi_0\rangle = |\uparrow_1\downarrow_2\rangle$, where the subscripts are regarding the charged dots, by turning on and off the bias voltage and anti-bias voltage repeatedly, we may have spin entanglement of the electrons in dots 1 and 2 after the following steps [23],

$$\begin{aligned}|\uparrow_1\downarrow_2\rangle &\to |\uparrow_A\downarrow_D\rangle \to (|\uparrow_A\downarrow_D\rangle + |\uparrow_B\downarrow_C\rangle)/\sqrt{2} \\ &\to (|\downarrow_A\uparrow_D\rangle + |\uparrow_B\downarrow_C\rangle)/\sqrt{2} \to (|\downarrow_1\uparrow_2\rangle + |\uparrow_1\downarrow_2\rangle)/\sqrt{2}, \end{aligned} \tag{1}$$

where the first step (denoted by the first right-pointed arrow) means the electron transition to A and D from 1 and 2, respectively. Then the electron tunneling under Coulomb repulsion yields the superposition of the 'charge polarization' states, i.e., entanglement regarding dots A, B, C, and D (see figure 2 and the discussion in appendix A). This charge entangled state could be exactly obtained by precisely controlling the bias electrode pulses [23, 25, 29]. The terms after the third right-pointed arrow account for the single-qubit flip made on sites A and D, for which an elaborate and fast operation is required, as discussed later. The fourth right-pointed arrow corresponds to the transition back to dots 1 and 2. For concision, we have omitted the product terms in the above equation regarding no electronic occupation. It is evident that, without direct spin–spin interaction involved, we may have spin entanglement of two electrons by using Coulomb interaction and electronic tunneling. The specific form of the prepared spin entanglement depends on the initial states $|\varphi_0\rangle$, the control of the tunneling and the individual spin operations.

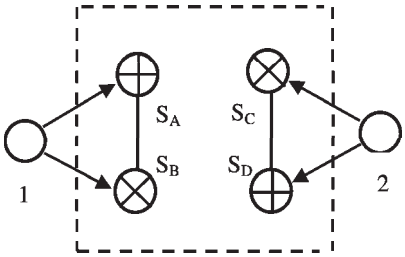

Figure 2. Production of superposition of charge polarization due to Coulomb repulsion, which corresponds to the first arrow in equation (1). The arrows mean the probability of transition to the dots A, B, C and D, and labels '×' and '+' in the circles account for the coherent occupation in diagonal sites and the counter-diagonal sites due to Coulomb repulsion. The label S_i with i = A, B, C and D means the spin of the electron on ith site. In our design, however, the spin–spin coupling is negligible compared to the Coulomb repulsion.

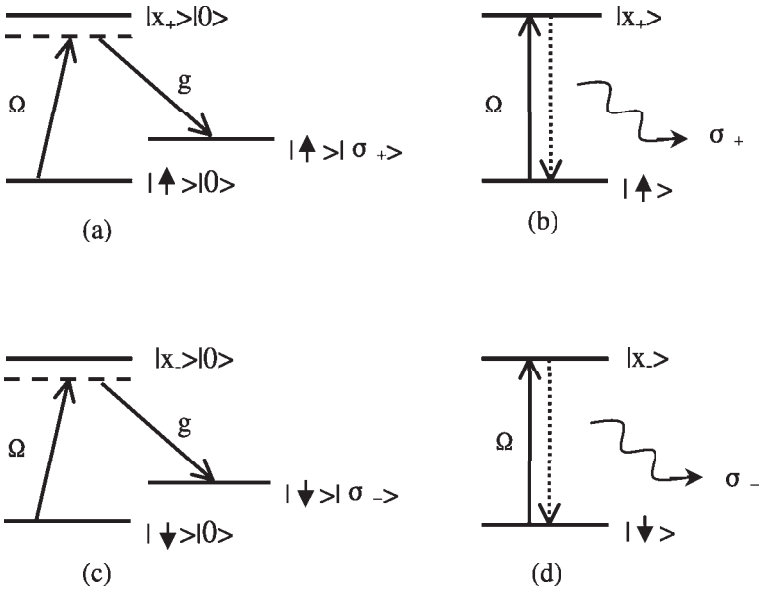

Figure 3. The generation of a single photon from a SQD 1 or 2. (a) and (c) correspond to the presence of the microcavities, in which we introduce a detuning for avoiding the spontaneous emission from the excitonic state, $|\cdot\rangle|\cdot\rangle$ means the product state of the dot and the cavity mode, and Ω and g denote, respectively, the transitions by the laser and the cavity. The photon produced is first absorbed by the microcavity, and then leaks away from one of the mirrors; (b) and (d) are for the situation in the absence of the microcavities, in which a transition in resonance is necessary, and we have to collect the photons generated from spontaneous emission.

To produce entangled photons, we have to employ excitons, whose production obeys the Pauli exclusion principle under polarized radiation [30], as shown in figure 3, where in the case of the single excess conduction band electron being up-polarized (i.e., $|\uparrow\rangle$), radiation of a σ_+ laser pulse would change $|1/2\rangle_{\text{con-e}}|-3/2\rangle_{\text{val-e}}|3/2\rangle_{\text{val-h}}$ to be $|X_+\rangle = |1/2\rangle_{\text{con-e}}|-1/2\rangle_{\text{con-e}}|3/2\rangle_{\text{val-h}}$, where the subscripts denote the conduction band electron (con-e), valence band electron (val-e), and valence band hole (val-h), respectively. The excitonic state $|X^+\rangle$ will soon decay back to $|1/2\rangle_{\text{con-e}}|-3/2\rangle_{\text{val-e}}|3/2\rangle_{\text{val-h}}$ with emission of a σ_+ polarized photon. Similarly, for a down-polarized (i.e., $|\downarrow\rangle$) electron in the conduction

band, radiation of a σ_- laser pulse yields $|X^-\rangle = |-1/2\rangle_{\mathrm{con-e}}|1/2\rangle_{\mathrm{con-e}}|-3/2\rangle_{\mathrm{val-h}}$ from $|-1/2\rangle_{\mathrm{con-e}}|3/2\rangle_{\mathrm{val-e}}|-3/2\rangle_{\mathrm{val-h}}$, which finally results in the emission of a σ_- photon[5]. Therefore, in our case, a radiation with both σ_+ and σ_- lights will lead to

$$\begin{aligned}(|\uparrow_1\downarrow_2\rangle + |\downarrow_1\uparrow_2\rangle)/\sqrt{2} &\rightarrow (|X_1^+X_2^-\rangle + |X_1^-X_2^+\rangle)|00\rangle_{\mathrm{I\,II}}/\sqrt{2} \\ &\rightarrow (|\uparrow_1\downarrow_2\rangle|\sigma_+\sigma_-\rangle_{\mathrm{I\,II}} + |\downarrow_1\uparrow_2\rangle|\sigma_-\sigma_+\rangle_{\mathrm{I\,II}})/\sqrt{2}, \end{aligned} \tag{2}$$

where we denote by $|\rangle_{\mathrm{I\,II}}$ the states of the two microcavities. To be concise, we have used $|i\rangle_j$ ($j = \mathrm{I}, \mathrm{II}$) to label the two modes of the jth cavity, with $i = \sigma_+$ or σ_-. Equation (2) is the simplest way to present the main steps of our implementation. Actually, in the presence of the microcavities, the excitonic terms between the two right-pointed arrows only exist virtually due to large detuning (see figures 3(a) and (c)), and the cavity decay yields probabilistic success, as demonstrated in appendix B.

To entangle the photons, we must have the electrons moving again by changing the bias and anti-bias voltages, which yields

$$\begin{aligned}\frac{1}{\sqrt{2}}(|\uparrow_1\downarrow_2\rangle|\sigma_+\sigma_-\rangle_{\mathrm{I\,II}} + |\downarrow_1\uparrow_2\rangle|\sigma_-\sigma_+\rangle_{\mathrm{I\,II}}) &\rightarrow \frac{1}{\sqrt{2}}(|\uparrow_{\mathrm{A}}\downarrow_{\mathrm{D}}\rangle|\sigma_+\sigma_-\rangle_{\mathrm{I\,II}} + |\downarrow_{\mathrm{A}}\uparrow_{\mathrm{D}}\rangle|\sigma_-\sigma_+\rangle_{\mathrm{I\,II}}) \\ &\rightarrow \frac{1}{\sqrt{2}}(|\uparrow_{\mathrm{A}}\downarrow_{\mathrm{D}}\rangle + |\uparrow_{\mathrm{B}}\downarrow_{\mathrm{C}}\rangle)|\sigma_+\sigma_-\rangle_{\mathrm{I\,II}} + \frac{1}{\sqrt{2}}(|\downarrow_{\mathrm{A}}\uparrow_{\mathrm{D}}\rangle + |\downarrow_{\mathrm{B}}\uparrow_{\mathrm{C}}\rangle)|\sigma_-\sigma_+\rangle_{\mathrm{I\,II}} \\ &\rightarrow \frac{1}{\sqrt{2}}(|\downarrow_{\mathrm{A}}\uparrow_{\mathrm{D}}\rangle + |\uparrow_{\mathrm{B}}\downarrow_{\mathrm{C}}\rangle)|\sigma_+\sigma_-\rangle_{\mathrm{I\,II}} + \frac{1}{\sqrt{2}}(|\uparrow_{\mathrm{A}}\downarrow_{\mathrm{D}}\rangle + |\downarrow_{\mathrm{B}}\uparrow_{\mathrm{C}}\rangle)|\sigma_-\sigma_+\rangle_{\mathrm{I\,II}} \\ &\rightarrow \tfrac{1}{2}(|\downarrow_1\uparrow_2\rangle + |\uparrow_1\downarrow_2\rangle)(|\sigma_+\sigma_-\rangle_{\mathrm{I\,II}} + |\sigma_-\sigma_+\rangle_{\mathrm{I\,II}}), \end{aligned} \tag{3}$$

where the first and the fourth right-pointed arrows account for the transitions between sites 1 (2) and the QCA, and the terms after the second right-pointed arrow indicate the tunneling within the QCA. The single-qubit flip occurs in the third step. It is evident that the modes of the two cavities are entangled in the last step, and we will have entangled photons after the photons leak out of the microcavities. Since the two electron spins are left in entanglement, if we want more entangled photons, we only need to repeat the steps in equations (2) and (3). How well we could produce entangled photons depends on the speed of our manipulation and decoherence time, as discussed later.

3. Discussion

3.1. Experimental availability

Some steps in our proposal have already been within the reach of current nanotechnologies. The optical generation of excitons has been available, based on which a controlled rotation was achieved in [31]. The experimental preparation of a single conduction band electron has been reported [32], and a very recent experiment has demonstrated single spin manipulation on the conduction band electron [33]. In addition, since the Coulomb repulsion instead of the spin–spin interaction yields the entanglement, the interdot distance could be relatively large, e.g., hundreds of nanometers, which makes the individual manipulation in our scheme relatively easier than in previous schemes based on purely spin–spin interaction, e.g., [30].

Since experiments for double QDs made of GaAs were carried out under charge-qubit operation [25, 26] and under coherent manipulation regarding electron spin [27], we may

[5] Here we consider III–V SQDs in which the heavy holes $|\pm 3/2\rangle_{\mathrm{val-h}}$ are the ground states. Alternatively, we may choose II–V SQDs by using the light holes $|\pm 1/2\rangle_{\mathrm{val-h}}$ to produce a charged excitonic state, as done in [30]. Moreover, the description here is more suitable for the situation in figures 3(b) and (d), while in the case of figures 3(a) and (c), the excitons are produced virtually.

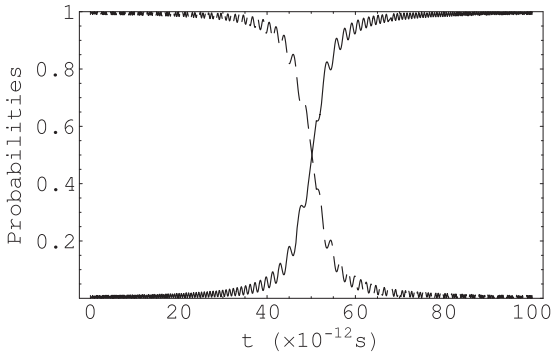

Figure 4. Probabilities of the electron in site 1 (dashed curve) and in site A (solid curve) with respect to time, where we assume the bias voltage to be varied linearly, as shown in the text.

assess our scheme by the values from them, although the ideas and the implementation in [25–27] are not identical to ours here. Assuming that the dot spacing d between A and B (or between C and D) is 300 nm [25, 27], to achieve our scheme, we have to satisfy a condition $Ke^2/r < E_{\text{bias}} < Ke^2/d$, where $K = 8.2 \times 10^8$ N m^2 C^{-2} accounts for Coulomb repulsion in GaAs, e is the single-electron charge, $r = \sqrt{2}d$, and E_{bias} is related to the external bias voltage. This condition ensures the evolution between the two charge polarization states, but prevents simultaneous occupation of electrons on sites A and C or B and D. Direct calculation shows that the Coulomb repulsion between the diagonal sites (e.g., A and D) is smaller than that between the side sites (e.g., A and B) by 0.16 meV, and the tunneling rate $\tilde{W}$ (defined in appendix A) by E_{bias} overcoming Coulomb repulsion could be about 0.2 terahertz. A preliminary experiment [29] at 100 mK has demonstrated the availability of the antipodal polarization in QCA with SQDs. We believe that the electron tunneling in QCA could be observed at lower temperature by using more elaborate operations.

To have a high-fidelity entangled state, however, we have to consider the whole process from the electrons initially polarized in sites 1 and 2 to their finally getting back to 1 and 2 in entanglement from the QCA, respectively. The transition between 1 (2) and a site of the QCA could be simulated by the well-known Landau–Zener model [34]. Suppose that the energy gap between site 1 (2) and A (D) is $\epsilon(t)$, which is adjustable by the bias voltage between the QCA and the site 1 (2), and the transition rate is R. We have

$$H_{\text{tran}} = \epsilon(t)(|1\rangle\langle 1| - |\text{A}\rangle\langle\text{A}|) + R(|1\rangle\langle\text{A}| + |\text{A}\rangle\langle 1|). \tag{4}$$

We assume $\epsilon(t) = \epsilon_0 - Vt$ with $\epsilon_0{:}R{:}V = 1{:}1/10{:}1/50$, and ϵ_0 is of the order of meV. Numerical calculation shows that such a transition takes 80 ps (see figure 4). Then the electrons will tunnel coherently within the QCA, whose dynamics is described in appendix A. The time for the two electrons becoming entangled in spin degrees of freedom is about $\pi/(4\tilde{W})$, and then the electrons move back to sites 1 and 2 from QCA sites. Due to symmetry, this returning time is also 80 ps.

With the bias voltage controlled, we could accomplish the steps in equation (1) within 164 ps. So considering equations (1), (2) and (3) together (i.e., with the excitonic lifetime 40 ps or with the implementation time 150 ps in cavities by virtually exciting excitons [30]), we could generate an entangled photon pair within 500 ps. As the charge entangled state in our proposal exists no longer than 164 ps, a high-quality charge entangled state seems available with current experimental techniques. For example, the experimental observation in [26] for the decoherence times of the charged qubit is $T_1 = 16$ ns and $T_2 = 400$ ps, both longer than the

time we need. As for the entanglement of electron spins in the conduction band of SQDs, the decoherence time was generally considered to be of the order of a nanosecond. It was estimated in [35] that the decoherence time could be 1 μs for the conduction band electron spin in GaAs SQDs embedded in AlGaAs. The observation in [27] also indicated that T_2 in GaAs/AlGaAs SQDs had reached 10 ns and T_1 could be as long as 1 μs, both of which are much longer than 500 ps.

As the decoherence time for electron spin is much longer than the implementation time, we may completely neglect the decoherence in this respect, while for charge entangled states, decoherence would somewhat damage the entanglement [36]. As discussed in [25], the sources of this decoherence are complicated, regarding background charge fluctuation and noise, electron–phonon interaction, low-frequency noise and so on. Although the decoherence mechanism is not fully clear, at lower temperature most of these decoherence effects would be suppressed. Moreover, by slightly increasing the tunneling rate R, the transition time in figure 4 would be possibly shorter than 30 ps. So a high-fidelity charge entangled state in our model is in principle available.

3.2. Experimental challenge

To achieve an exciton governed by the Pauli exclusion principle, we require the electron to stay in the ground state of the conduction band. To do this, we may consider a very shallow conduction band with only a single discrete level. In this case, however, we have to prevent the electron from escaping. So the required temperature should be very low, e.g., below 20 mK, as in [25]. Moreover, we have noticed that there is no spin involved in the transition experiment [25, 26, 29]. However, due to the independence of charge and spin degrees of freedom, we assume that the same experimental device as in [25, 26, 29] should enable a coherent tunneling of a polarized electron. In fact, this assumption has been used in previous work [22–24]. Furthermore, we have mentioned that the SQDs embedded in microcavities could collect the generated photons with much higher rate than the case of spontaneous emission. But the case of three SQDs in a microcavity with strong coupling has not yet been reported experimentally, although it is in principle possible with a microdisc-like cavity [35]. Nevertheless, the coupling of the cavity modes to the electron spins occurs only when the electrons stay in dots 1 and 2. In this sense, we may simply consider the case with a single dot in a microcavity and estimate the success rate of the entangled photon generation. Since we could neglect the electron–spin decoherence, if we also omit other imperfect factors, the cavity decay is the dominant error source in current experiment [37]. As shown in appendix B and also in figure 5, a high-quality cavity with $\kappa \leqslant \tilde{\Omega}/1000$ (defined in appendix B) is essential to the high efficiency of the entangled photon generation. On the other hand, without microcavities, our scheme could still work well in production of the generated photons, while the collection rate of generated photons would be low due to spontaneous emission and the finite-angle coverage of the collector[6]. It should be emphasized that the successful collection of the two generated photons is evidence of the success of our implementation. As there is no spin detection (or say, no post-selection) in the generation of entangled photons in our scheme, we do not have a step to filter out the failure case. Nevertheless, as shown in appendix B, only in the case of a successful implementation do we have two photons leaking out of the cavities. So collection of photons is very important to the implementation of our proposal.

As the tunneling rate is 200 GHz, fast but accurate manipulation is highly required. The operational imperfection probably occurs due to imprecise switch of the bias voltage or to the slight difference of the SQDs. We may consider the effects from these imperfect factors to be a

[6] Some discussions in this respect were made in Calarco *et al* [38]. Also see an experiment for collecting photons from spontaneous emission of a trapped atom with the collection rate lower than 2% [39].

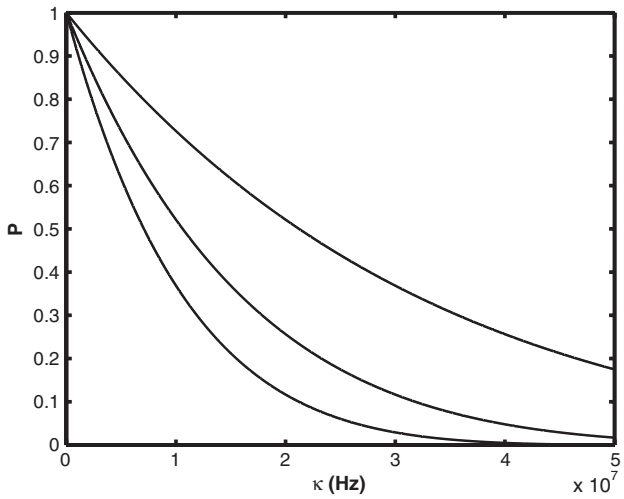

Figure 5. Success rate P of the generated entangled photon pairs versus the cavity decay rate κ, where we assume in the calculation $g = \Omega = 1$ GHz, and the curves from the top to bottom correspond to $\Delta = 10, 20, 30$ GHz. The larger detuning results in a better approximation of the effective Hamiltonian in appendix B, although it leads to a lower success rate.

time delay δt resulted by different switch time or different gap energies[7]. This would yield the final entangled state between dots 1 and 2 to be $\cos(\pi/4+\delta)|\downarrow_1\uparrow_2\rangle + \sin(\pi/4+\delta)|\uparrow_1\downarrow_2\rangle$, where $\delta = \tilde{W}\delta t$ is due to undesired tunneling or transition regarding δt. So the fidelity would be $\cos^2\delta$. This implies that, to achieve our proposal with a fidelity higher than 98%, the time delay δt should be smaller than 0.7 ps. To this end, exact knowledge of each SQD is necessary and we are required to design specifically fast and accurate sequences of the bias voltages for different tunnelings or transitions.

Also, because of the fast tunneling, the single-qubit operation has to be accomplished within a time shorter than 10^{-11} s. Fortunately, we have found an experiment for fast single-spin rotation by ultrafast optical pulses at the timescale of a femtosecond [39]. Although this was done in a quantum well, instead of in a SQD, this experiment gives us a hope to carry out our scheme with high fidelity.

Furthermore, individually addressing with lasers for nanoscale spaced SQDs is still challenging with currently techniques. To overcome this difficulty, one has to employ different SQDs and a near-field technique based on the exact knowledge of each SQD, which is the idea widely adopted in almost all proposals with SQDs for quantum information processing. We may also use this idea in our scheme here. As the spacing of the neighboring dots in our case could be hundreds of nanometers, individually addressing with lasers should be much easier than previous schemes involving spin–spin dipolar interaction.

3.3. Problems regarding measurement

In current experiments, it is difficult to measure a single-electron spin. The experiments that have been achieved and most proposals are based on the transfer to the electric signal from the

[7] We assume the SQDs to be nearly identical in our treatment. Although there are no identical SQDs in nature, we may take two SQDs to be almost identical if their difference is too small for us to distinguish and is not reflected in the tunneling and the transition. This assumption was evidenced in the experiments [25, 29]. On the other hand, we may also resort the slight difference of SQDs to the imperfect factor δt due to difference energy gap or SQD shape, as done in [36].

information of the spin. For example, in a recent experiment [40], the spin polarization of an excess conduction band electron was detected by moving the electron away by quantum point contact, which yields a detectable electric signal due to single-electron jump. But this operation actually destroys the system, instead of merely quantum collapse, which is not practical in real quantum computing. In contrast, as the final result in equation (3) is a product state consisting of electron spin and photon polarization, we do not need any detection to yield the photon entanglement. So although the nondestructive detection of the single-electron spin in a SQD has been available very recently by an optical method [41], our scheme without the need of measurement makes the implementation simpler.

On the other hand, indistinguishability is preferred for the entangled photons in some quantum information processing tasks, e.g., in the linear optical proposal with additional off-line source of entangled identical photons [15]. The entanglement of different-energy photons is easily lost in interaction with matter (e.g., detectors or atoms). In this sense, once future technique could enable one to produce two nearly identical SQDs to be dots 1 and 2, two almost identical photons in entanglement could be generated by our scheme, which is impossible for biexciton ideas.

4. Conclusion

In summary, we have proposed a unique scheme to generate entangled photons by SQDs in a structure of QCA. Although this is still highly challenging to be achieved with current experimental techniques, our scheme, as discussed above, would be a good design for near-future techniques to generate entangled photon pairs deterministically, repeatedly, and efficiently. In comparison with relevant proposals published previously, our scheme has advantages in some practical aspects: no level splitting due to asymmetry in biexcitonic decay, no spin–spin interaction required, and reachable high fidelity for entangled photon pairs. Also, as it involves the idea of an electron charge independent from its spin degrees of freedom, our scheme would be not only for a source of entangled photon pairs, but also applicable to other quantum information processing tasks with free electrons.

Acknowledgments

MF gratefully acknowledges the support by the National Natural Science Foundation of China under contract No. 10474118 and by Hubei Provincial Funding for Distinguished Young Scholars. This work is also partially supported by National Science Council of ROC under contract No. NSC-94-2120-M-006-003, No. NSC-95-2112-M-006-001, National Center for Theoretical Science No. NSC-95-2119-M-006-001, and NNSFC No. 10604025.

Appendix A. Production of entangled charge states by Coulomb repulsion

Although the main points have been presented in [19, 23], we would like to give a more detailed description below for the electron tunneling within QCA. We denote by R_{ij} the transition rate from dot i to dot j. As discussed in section 3.1, by adjusting the bias voltages, we make $R_{1A} = R_{2D} \gg R_{1B} \approx R_{2C}$, which yields almost with certainty the state $|\uparrow_A\downarrow_D\rangle$ after the transition. Please keep in mind that we are considering a model with spin coupling that is negligible due to large interdot spacing, and thereby the charge degrees of freedom, due to Coulomb repulsion, play the dominant role. The spins labeled in above state vector are just for coinciding with equation (1). After the electrons are transited into dots A and D, the large

energy gap between the site 1 (2) and the site inside the QCA restricts the electrons to moving only within the cells. Then we may consider the following effective Hamiltonian of the QCA,

$$H_{\text{eff}} = \tilde{W}(|\uparrow_{\text{A}}\downarrow_{\text{D}}\rangle\langle\uparrow_{\text{B}}\downarrow_{\text{C}}| + |\uparrow_{\text{B}}\downarrow_{\text{C}}\rangle\langle\uparrow_{\text{A}}\downarrow_{\text{D}}|),$$

where we have used the notion of coherent tunneling of the 'charge polarization' [19, 23], and $\tilde{W}$ is the effective tunneling rate of the coupled dots AB and CD in the QCA, which meets the condition mentioned in section 3. Note that H_{eff} above is actually from a second-order perturbative calculation of the original QCA Hamiltonian, which includes the on-site energy of each dot, electron tunneling between neighboring dots, on-site energy of double electrons in each dot, and Coulombic interaction between electrons on different sites[8]. So $\tilde{W}$ is proportional to the square of the tunneling rate between vertically neighboring dots. For $|\varphi(0)\rangle = |\uparrow_{\text{A}}\downarrow_{\text{D}}\rangle$, we have

$$|\varphi(t)\rangle = \cos(\tilde{W}t)|\uparrow_{\text{A}}\downarrow_{\text{D}}\rangle - \text{i}\sin(\tilde{W}t)|\uparrow_{\text{B}}\downarrow_{\text{C}}\rangle.$$

We have, at the evolution time $t_1 = (2m\pi + \pi/4)/\tilde{W}$ (m being an integer), the state $|\varphi(t_1)\rangle = (|\uparrow_{\text{A}}\downarrow_{\text{D}}\rangle - i|\uparrow_{\text{B}}\downarrow_{\text{C}}\rangle)/\sqrt{2}$. Since $\tilde{W}$ is known, the current state-of-the-art laser technique could enable us to remove the prefactor $(-\text{i})$ from the component $|\uparrow_{\text{B}}\downarrow_{\text{C}}\rangle$ by a polarization $\pi/2$-pulse [23]. So at the exact time $t = t_1$, we could reach $|\varphi(t_1)\rangle = (|\uparrow_{\text{A}}\downarrow_{\text{D}}\rangle + |\uparrow_{\text{B}}\downarrow_{\text{C}}\rangle)/\sqrt{2}$, as shown in equation (1). As this could be accomplished within the timescale of femtoseconds, much shorter than the tunneling time, the above single-spin operation costs negligible time in our case. So following another single-spin operation to flip the electron spins, i.e., $|\uparrow\rangle(|\downarrow\rangle) \rightarrow |\downarrow\rangle(|\uparrow\rangle)$, on sites A and D, we reach $|\varphi(t_1)\rangle = (|\downarrow_{\text{A}}\uparrow_{\text{D}}\rangle + |\uparrow_{\text{B}}\downarrow_{\text{C}}\rangle)/\sqrt{2}$. This implies that, at time $t = t_1$, we may turn on the bias voltage to transit the electrons in $|\varphi(t_1)\rangle$ back to the dots 1 and 2. This treatment is also applicable to the relevant steps in equation (3).

Appendix B. Production of entangled photon pairs under cavity dissipation

In a recent experiment [37] for a single SQD embedded in a microcavity and strongly coupled to the cavity mode, the cavity decay rate is of the same order of 10^{11} Hz as the coupling strength. So we consider the cavity decay to be the main dissipative factor, which affects the success rate of our scheme. The large detuning Δ yields an effective Rabi frequency $\tilde{\Omega} = |\Omega| \cdot g/\Delta$ with Ω and g the couplings due to the laser and the cavity, respectively. For clarity, we label the levels in figures 3(a) and (c) regarding $|\uparrow\rangle|0\rangle$, $|\uparrow\rangle|\sigma_+\rangle$, $|\downarrow\rangle|0\rangle$, and $|\downarrow\rangle|\sigma_-\rangle$ by $|E_1\rangle$, $|E_2\rangle$, $|E_3\rangle$, and $|E_4\rangle$, respectively. In the case of $|\Omega| \ll \Delta$ and $g \ll \Delta$, we have an effective Hamiltonian,

$$H = \sum_{m=1}^{2} \tilde{\Omega}(a_m^\dagger|E_2\rangle_m\langle E_1| + a_m|E_1\rangle_m\langle E_2| + b_m^\dagger|E_4\rangle_m\langle E_3| + b_m|E_3\rangle_m\langle E_4|)$$
$$- \text{i}\kappa\sum_{m=1}^{2}(a_m^\dagger a_m + b_m^\dagger b_m),$$

where $m = 1, 2$ regarding the dots 1 and 2, respectively, $a^\dagger(a)$ and $b^\dagger(b)$ create (annihilate) σ_+ and σ_- polarized photons, respectively, and κ is for the decay rate. For simplicity, we consider the effective Rabi frequency and the decay rate to be constant for different modes and dots. To produce high-quality entangled photons, we require the photon decay from the microcavity not to happen during the scheme implementation. As a result, we would solve the time evolution

[8] Compared to equation (6) in Toth and Lent's paper [19], only the tunneling term remains in H_{eff}. This is because we consider a zero on-site energy case, which is achievable by decreasing the local potential of each dot when switching on the bias for tunneling.

of the system straightforwardly by the same technique used before [42]. Starting from the entangled state,

$$|\Psi_0\rangle = (|E_1\rangle_1|E_3\rangle_2 + |E_3\rangle_1|E_1\rangle_2)/\sqrt{2},$$

we have

$$|\Psi(\tau_0)\rangle = \frac{1}{M}\mathrm{e}^{-\kappa\tau_0}\left[\frac{\kappa^2}{\Omega'^2}(|E_1\rangle_1|E_3\rangle_2 + |E_3\rangle_1|E_1\rangle_2) - \frac{4\tilde{\Omega}^2}{\Omega'^2}(|E_4\rangle_1|E_2\rangle_2 + |E_2\rangle_1|E_4\rangle_2)\right.$$
$$\left. - \frac{2\mathrm{i}\tilde{\Omega}\kappa}{\Omega'^2}(|E_1\rangle_1|E_4\rangle_2 + |E_3\rangle_1|E_2\rangle_2 + |E_2\rangle_1|E_3\rangle_2 + |E_4\rangle_1|E_1\rangle_2)\right],$$

where $M = \sqrt{2}(4\tilde{\Omega}^2 + \kappa^2)/\Omega'^2$, $\Omega' = \sqrt{4\tilde{\Omega}^2 - \kappa^2}$, and $\tau_0 = \pi/\Omega'$. If $\kappa = 0$, $|\Psi(\tau_0)\rangle$ reduces to $|\Psi_1\rangle = (|E_4\rangle_1|E_2\rangle_2 + |E_2\rangle_1|E_4\rangle_2)/\sqrt{2} = (|\downarrow\uparrow\rangle|\sigma_-\sigma_+\rangle + |\uparrow\downarrow\rangle|\sigma_+\sigma_-\rangle)/\sqrt{2}$, and the photons will stay in the microcavity forever. As κ is not zero for a real cavity, we only have the success probability

$$P = 16\mathrm{e}^{-2\kappa\tau_0}\tilde{\Omega}^4/(4\tilde{\Omega}^2 + \kappa^2)^2,$$

to obtain $|\Psi_1\rangle$, as shown in figure 5.

References

[1] Aspect A, Grangier P and Roger G 1982 *Phys. Rev. Lett.* **49** 91
[2] Kwiat P G, Mattle K, Weinfurter H, Zeilinger A, Sergienko A V and Shih Y H 1995 *Phys. Rev. Lett.* **75** 4337
[3] Shih Y H and Alley C O 1988 *Phys. Rev. Lett.* **61** 2921
[4] Bensen O, Santori C, Pelton M and Yamamoto Y 2000 *Phys. Rev. Lett.* **84** 2513
[5] Stace T M, Milburn G J and Barnes C H W 2003 *Phys. Rev.* A **67** 085317
[6] Edamatsu K, Oohata G, Shimizu R and Itoh T 2004 *Nature* **431** 167
[7] Cerletti V, Gywat O and Loss D 2005 *Phys. Rev.* B **72** 115316
[8] Titov M, Trauzettel B, Michaelis B and Beenakker C W J 2005 *New J. Phys.* **7** 186
[9] Simon C and Poizat J-P 2005 *Phys. Rev. Lett.* **94** 030502
[10] Akopian N, Lindner N H, Poem E, Berlatzky Y, Avron J and Gershoni D 2006 *Phys. Rev. Lett.* **96** 130501
[11] Stevenson R M, Young R J, Atkinson P, Cooper K, Ritchie D A and Shields A J 2006 *Nature* **439** 179
[12] Bouwmeester D, Pan J W, Mattle K, Eibl M, Weinfurter H and Zeilinger A 1997 *Nature* **390** 575
[13] Pan J W, Simon C, Brukner C and Zeilinger A 2001 *Nature* **410** 1067
[14] Zhao Z, Chen Y A, Zhang A N, Yang T, Briegel H J and Pan J W 2005 *Nature* **430** 54
[15] Knill E, Laflamme R and Milburn G J 2001 *Nature* **409** 46
[16] For example, Plenio M B, Huelga S F, Beige A and Knight P L 1999 *Phys. Rev.* A **59** 2468
Sorensen A S and Molmer K 2003 *Phys. Rev. Lett.* **90** 12703
[17] Duan L-M and Kimble H J 2003 *Phys. Rev. Lett.* **90** 253601
[18] Chou C W, Riedmatten H de, Felinto D, Polyakov S V, Enk S J and van Kimble H J 2005 *Nature* **438** 828
[19] Toth G and Lent C S 2001 *Phys. Rev.* A **63** 052315
[20] Kiraz A *et al* 2002 *Phys. Rev.* B **65** 161303(R)
Zwiller V *et al* 2002 *Phys. Rev.* A **66** 053814
Stevenson R M *et al* 2002 *Phys. Rev.* B **66** 081302
[21] Santori C, Fattal D, Pelton M, Solomon G S and Yamamoto Y 2002 *Phys. Rev.* B **66** 045308
[22] Beenakker C W J, DiVincenzo D P, Emary C and Kindermann M 2004 *Phys. Rev. Lett.* **93** 020501
[23] Zhang W M, Wu Y Z and Soo C 2005 *Preprint* quant-ph/0502002
Wu Y Z and Zhang W M 2005 *Europhys. Lett.* **71** 524
[24] Engel H A and Loss D 2005 *Science* **309** 586
[25] Hayashi T, Fujisawa T, Cheong H D, Jeong Y H and Hirayama Y 2003 *Phys. Rev. Lett.* **91** 226804
[26] Petta J R, Johnson A C, Marcus C M, Hanson M P and Gossard A C 2004 *Phys. Rev. Lett.* **93** 186802
[27] Petta J R, Johnson A C, Taylor J M, Laird E A, Yacoby A, Lukin M D, Marcus C M, Hanson M P and Gossard A C 2007 *Science* **309** 2180
[28] Orlov A O, Amlani I, Bernstein G H, Lent C S and Snider G L 1997 *Science* **277** 928
Orlov A O *et al* 1999 *Appl. Phys. Lett.* **74** 2875
Amlani I *et al* 1999 *Science* **284** 289

[29] Gardelis S, Smith C G, Cooper J, Ritchie D A, Linfield E H and Jin Y 2003 *Phys. Rev.* B **67** 033302
[30] Feng M, D'Amico I, Zanardi P and Rossi F 2003 *Phys. Rev.* A **67** 014306
Feng M, D'Amico I, Zanardi P and Rossi F 2004 *Europhys. Lett.* **66** 14
[31] Li X, Wu Y, Steel D, Gammon D, Stievater T H, Katzer D S, Park D, Piermarocchi C and Sham L J 2003 *Science* **301** 809
[32] Finley J J, Skalitz M, Arzberger M, Zrenner A, Boehn G and Abstreiter G 1998 *Appl. Phys. Lett.* **73** 2618
[33] Kroutvar M, Ducommun Y, Heiss D, Bichler M, Schuh D, Abstreiter G and Finley J J 2004 *Nature* **432** 81
[34] Landau L D 1932 *Phys. Z. Sowjetunion* **2** 46
Zener C 1932 *Proc. R. Soc.* A **137** 696
[35] Imamoglu A, Awschalom D D, Burkard G, DiVincenzo D P, Loss D, Sherwin M and Small A 1999 *Phys. Rev. Lett.* **83** 4204
[36] Contreras-Pulido L D and Rojas F 2006 *J. Phys.: Condens. Matter* **18** 9771
[37] Reithmaier J P, Sek G, Loffler A, Hofmann C, Kuhn S, Reitzenstein S, Keldysh L V, Kulakovskii V D, Reinecke T L and Forchel A 2004 *Nature* **432** 197
[38] Calarco T *et al* 2003 *Phys. Rev.* A **68** 012310
Blinov B B, Moehring D L, Duan L-M and Monroe C 2004 *Nature* **428** 153
[39] Gupta J A, Knobel R, Samarth N and Awschalom D D 2001 *Science* **292** 2458
[40] Elzerman J M, Hanson R, Beveren L H, Willems van, Witkamp B, Vandersypen L M K and Kouwenhoven L P 2004 *Nature* **430** 431
[41] Berezovsky J, Mikkelsen M H, Gywat O, Stoltz N G, Coldren L A and Awschalom D D 2006 *Science* **314** 1916
[42] Feng M, Deng Z J and Gao K L 2005 *Phys. Rev.* A **72** 042333